Conductive Block Copolymers Integrated into Polynorbornene-Derived Scaffolds

Hyun A Kang, Hindy E. Bronstein, and Timothy M. Swager*

Department of Chemistry, Massachusetts Institute of Technology, 77 Massachusetts Avenue, Cambridge, Massachusetts 02139

Received March 23, 2008; Revised Manuscript Received May 27, 2008

ABSTRACT: The synthesis and electrochemical properties of novel block copolymers are reported. Three different norbornene derivatives having phenylene−thiophene, phenylene−bithiophene, and phenylene−furan structures were copolymerized with either norbornene or 7-oxanorbornene derivatives via ring-opening metathesis polymerization (ROMP). Block copolymers' stabilities and solubilities could be improved by hydrogenation of double bonds in the polymer backbone. The block copolymers were subsequently cross-linked by anodic electropolymerization of phenylene−heterocycle moieties, affording conducting polymers. All of these three block copolymers were readily deposited on the electrode substrates, and their cyclic voltammograms (CVs) revealed an excellent reversibility in the redox cycles.

Introduction

Conducting polymers (CPs) continue to receive broad attention due to expanding applications possibilities resulting from their electronic and optical properties.[1] Of the many interesting CPs, those based on poly(*p*-phenylene), polypyrrole, and polythiophene backbones have been studied the most since they are chemically and electronically stable in both the oxidized and neutral states.[2] These CPs are generally synthesized via chemical or electrochemical polymerizations that proceed by a step growth mechanism. Although electrochemical syntheses of CPs are convenient methods, there are several limitations to this approach such as low yields, low processability, and complex morphologies.[3,4] One approach to overcome these limitations is the use of precursor polymers having pendant electroactive moieties.[4,5] In previous investigations, processable precursor polymers obtained from ROMP,[6] which can provide controlled molecular weights, produced high-quality CPs after oxidative cross-linking. Most recently, the Sotzing group has developed a solid-state oxidative cross-linking (SOC) technique in which a precursor polymer containing pendant terthiophene prepared by ROMP was electropolymerized in the solid swollen state.[3] An advantage of the SOC technique is to afford more highly conjugated CPs than conventional electrochemical polymerization, and this technique was applied to the fabrication of plastic nanoscale electronic devices using scanning probe-based lithography.[7]

The tendency of the block copolymer blocks to phase-separate can result in self-assembly of these electronic polymers into a variety of nanoscale structures.[8] Well-defined nanostructures of conducting polymers are especially attractive because controlled structures are needed to optimize numerous applications. Toward this end, we have designed new precursor monomers with a two point fused phenylene ring to force coalignment of CP backbone with the initial backbone produced by ROMP (Scheme 1). In this paper, we report conjugated block copolymers synthesized from three different norbornene derivatives having phenylene−thiophene, phenylene−bithiophene, and phenylene−furan structures. The polynorbornene backbone is a choice structure because of its flexibility, low glass transition temperature, inertness to electrochemical side reactions,[9] and ease of preparation via living ROMP.[10]

* Corresponding author: e-mail tswager@mit.edu.

Scheme 1

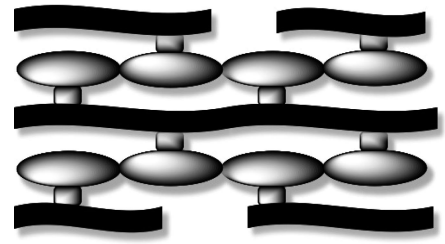

Experimental Section

Instrumentation. NMR spectra were recorded on Varian Unity 300 MHz, Varian Mercury 300 MHz, or Varian Inova 500 MHz spectrometer. Chemical shifts were reported in ppm and referenced to residual NMR solvent peaks. Mass spectra (MS) were obtained at the MIT Department of Chemical Instrumentation Facility (DCIF) using Bruker Daltonics APEX II 3T FT-ICR-MS. Number-average molecular weight (M_n) and polydispersity index (PDI) of polymers were obtained on a HP series 1100 gel permeation chromatography (GPC) system in THF and calibrated with polystyrene standards. Glass transition temperature (T_g) was determined using a TA Instruments Q100 differential scanning calorimetry (DSC) at scan rate of 10 °C/min in nitrogen atmosphere. Electrochemical studies were performed using an Autolab PGSTAT 20 potentiostat (Eco Chemie) in a three-electrode cell consisting of a Pt button (1.6 mm diameter) or indium tin oxide (ITO)-coated glass (100 Ω sheet resistance) working electrode, a Pt wire counter electrode, and a Ag wire reference electrode in contact with 0.01 M $AgNO_3$/0.1 M $TBAPF_6$ in anhydrous solvent. The ferrocene/ferrocenium (Fc/Fc^+) redox couple was used as a reference. Spectroelectrochemistry was performed under ambient laboratory conditions on polymer films electrodeposited onto ITO-coated glass electrodes using Agilent 8453 UV−vis spectrophotometer.

Materials. CH_2Cl_2 and THF were purified by passage through solvent purification columns containing activated alumina. *N,N*-Dimethylformamide (DMF) was distilled from magnesium sulfate and stored over 4 Å molecular sieves. Tetrabutylammonium hexafluorophosphate ($TBAPF_6$) was recrystallized from ethanol. 5-Tributylstannyl-2,2′-bithiophene[11] and *exo*-5,6-dimethoxymethyl-7-oxabicyclo[2.2.1]hept-2-ene (**9**)[12] were prepared according to the literature procedure. All other reagents were used without further purification unless otherwise noted.

1,4-Dihydro-1,4-methanonaphthalene-5,8-dinonaflate (3). 1,4,4a,8a-Tetrahydro-1,4-methanonaphthalene-5,8-dione (**1**) (10.46 g, 60 mmol) was added to a solution of sodium hydroxide (5 g, 125

10.1021/ma8006416 CCC: $40.75
Published on Web 07/01/2008

Scheme 2

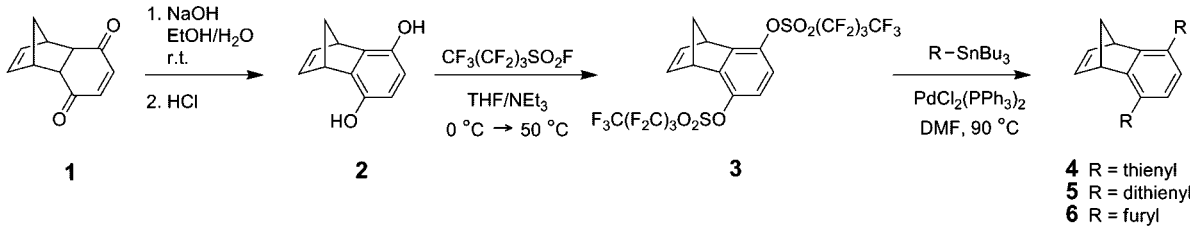

Scheme 3

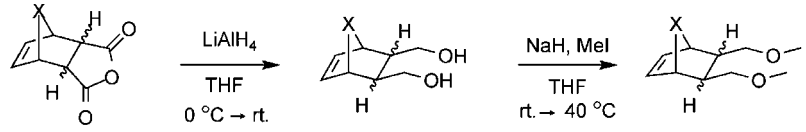

mmol) in ethanol (120 mL) and water (120 mL). The mixture was stirred at room temperature for 15 min, and then 5% HCl was added to acidify the solution. The mixture was extracted with ether and the organic portions were combined, washed with brine, dried over magnesium sulfate, and filtered. The crude mixture was obtained as a black powder (10.335 g). Crude compound **2** (7.15 g, 41 mmol) was dissolved in dry THF (160 mL), and the solution was cooled in an ice bath under argon. Trimethylamine (11 mL, 80 mmol) and perfluoro-1-butanesulfonyl fluoride (18.0 mL, 100 mmol) were added into the solution. The reaction mixture was brought to room temperature and stirred for 7 h. The solution was diluted with CH_2Cl_2 and washed with 5% HCl and brine. After drying over magnesium sulfate, the solution was filtered and the solvent was removed. The solid powder was loaded onto a short silica gel column and flushed with 10% CH_2Cl_2 in hexane, giving pure **3** (14.6 g, 48%) as a clear oil. ^{1}H NMR (300 MHz, $CDCl_3$): δ 6.93 (s, 2H), 6.88 (t, 2H, J = 1.8 Hz), 4.29−4.26 (m, 2H), 2.40 (dt, 1H, J = 7.8 Hz, J = 1.6 Hz), 2.34 (dt, 1H, J = 7.8 Hz, J = 1.7 Hz). ^{13}C NMR (75 MHz, $CDCl_3$): δ 148.12, 142.78, 120.16, 69.32, 49.03. ^{19}F NMR (188 MHz, $CDCl_3$): δ −81.07, −109.56, −121.26, −126.28. HR-MS (ESI): calcd for $C_{19}H_8F_{18}O_6S_2$ $[M + Na]^+$, 760.937; found 760.938.

5,8-Di(2-thienyl)-1,4-dihydro-1,4-methanonaphthalene (4). Compound **3** (9.687 g, 13.1 mmol) and 2-(tributylstannyl)thiophene (10 mL, 31.5 mmol) were dissolved in DMF (80 mL) under argon. Dichlorobis(triphenylphosphine) palladium(II) (462 mg, 0.66 mmol) was then added, and the reaction mixture was heated at 90 °C. After stirring for 12 h, the mixture was cooled to room temperature, diluted with ether, and washed with brine. After drying over magnesium sulfate, the solution was filtered, and the solvent was distilled off under reduced pressure. Column chromatography of the crude material on silica gel (5% CH_2Cl_2 in hexanes) provided the product as a white solid (2.87 g, 71%). The final purification was achieved by recrystallization from CH_2Cl_2/hexane; mp 120−121 °C. ^{1}H NMR (300 MHz, $CDCl_3$): δ 7.36 (dd, 2H, J = 5.1 Hz, J = 1.1 Hz), 7.22 (dd, 2H, J = 3.5 Hz, J = 1.1 Hz), 7.16 (s, 2H), 7.14 (dd, 2H, J = 3.6 Hz, J = 5.1 Hz), 6.98 (t, 2H, J = 1.8 Hz), 4.44−4.43 (m, 2H), 2.31−2.25 (m, 2H). ^{13}C NMR (75 MHz, $CDCl_3$): δ 150.04, 143.27, 142.75, 128.12, 127.79, 125.35, 125.32, 125.22, 69.16, 49.92. HR-MS (EI): calcd for $C_{19}H_{14}S_2$ $[M]^+$, 306.053; found 306.054.

5,8-Di(2-dithienyl)-1,4-dihydro-1,4-methanonaphthalene (5). This compound was synthesized by the same procedure as described for compound **4** using the following quantities of reagents: **3** (3.025 g, 4.1 mmol), 5-(tributylstannyl)-2,2′-bithiophene (4.84 g, 10.6 mmol), dichlorobis(triphenylphosphine) palladium(II) (141 mg, 0.20 mmol), and DMF (30 mL). Purification by column chromatography (silica gel, 5% CH_2Cl_2 in hexane) provided the product as a yellow solid (1.76 g, 91%). The final purification was achieved by recrystallization from CH_2Cl_2/ethanol; mp 183 °C. ^{1}H NMR (300 MHz, $CDCl_3$): δ 7.27 (dd, 2H, J = 5.1 Hz, J = 1.2 Hz), 7.25 (dd, 2H, J = 3.6 Hz, J = 1.2 Hz), 7.22 (d, 2H, J = 3.8 Hz), 7.17 (s, 2H), 7.16 (d, 2H, J = 3.8 Hz), 7.07 (dd, 2H, J = 3.7 Hz, J = 5.1 Hz), 7.01 (t, 2H, J = 1.8 Hz), 4.50−4.48 (m, 2H), 2.32 (dt, 1H, J = 7.3 Hz, J = 1.7 Hz), 2.26 (dt, 1H, J = 7.3 Hz, J = 1.5 Hz). ^{13}C NMR (75 MHz, $CDCl_3$): δ 150.07, 143.24, 141.59, 137.55, 137.33, 128.10, 127.89, 126.09, 124.93, 124.63, 124.48, 123.87, 69.19, 49.98. HR-MS (EI): calcd for $C_{27}H_{18}S_4$ $[M]^+$, 470.029; found 470.028.

5,8-Di(2-furyl)-1,4-dihydro-1,4-methanonaphthalene (6). This compound was synthesized by the same procedure as described for compound **4** using the following quantities of reagents: **3** (5.953 g, 8.06 mmol), 2-(tributylstannyl)furan (6.1 mL, 19.4 mmol), dichlorobis(triphenylphosphine)palladium(II) (286 mg, 0.41 mmol), and DMF (50 mL). Purification by column chromatography (silica gel, 5% CH_2Cl_2 in hexane) provided the product as a white solid (2.15 g, 90%). The final purification was achieved by recrystallization from ethanol; mp 118 °C. ^{1}H NMR (300 MHz, $CDCl_3$): δ 7.52 (dd, 2H, J = 1.8 Hz, J = 0.8 Hz), 7.26 (s, 2H), 6.92 (t, 2H, J = 1.8 Hz), 6.63 (dd, 2H, J = 3.4 Hz, J = 0.8 Hz), 6.51 (dd, 2H, J = 3.4 Hz, J = 1.8 Hz), 4.57−4.55 (m, 2H), 2.31 (dt, J = 7.3 Hz, J = 1.7 Hz), 2.25 (dt, J = 7.3 Hz, J = 1.6 Hz). ^{13}C NMR (75 MHz, $CDCl_3$): 153.89, 148.87, 143.25, 142.03, 124.22, 122.18, 111.67, 106.79, 68.47, 49.66. HR-MS (EI): calcd for $C_{19}H_{14}O_2$ $[M]^+$, 274.099; found 274.099.

***endo*-5,6-Bis(methoxymethyl)bicyclo[2.2.1]hept-2-ene (12).** This compound was synthesized using a method adapted from the preparation of compound **9**.[12] A solution of *endo*-bicyclo[2.2.1]hept-ene-2,3-dicarboxylic acid anhydride (**10**) (25 g, 152 mmol) in THF (120 mL) was added slowly to a suspension of lithium aluminum hydride (7.21 g, 190 mmol) in THF (200 mL) under argon at 0 °C. Then the reaction mixture was stirred at room temperature for 18 h. After the same work-up procedure that was used for the preparation of **9**,[12] the crude product (**11**) was obtained as a white solid (18.55 g, 79%). Diol **11** (19.70 g, 127 mmol) in THF (130 mL) was added slowly to sodium hydride suspension (16.5 g, 60% in mineral oil, 413 mmol) in THF (200 mL) under argon, and the mixture was stirred for 1 h. Methyl iodide (30 mL, 481 mmol) was added slowly. The reaction mixture was stirred for 1 h at room temperature and another 3 h at 40 °C and then cooled to room temperature. After neutralization, it was extracted with diethyl ether and washed with water. The solution was dried over magnesium sulfate and filtered, and the solvent was removed. The crude product was vacuum distilled from sodium to give a clear oil (18.65 g, 80%). ^{1}H NMR (300 MHz, $CDCl_3$): δ 6.10 (t, 2H, J = 1.8 Hz), 3.60 (s, 6H), 3.18−2.94 (m, 4H), 2.88 (m, 2H), 2.47−2.37 (m, 2H), 1.44 (dt, 1H, J = 8.3 Hz, J = 1.8 Hz), 1.28 (d, 1H, J = 8.3 Hz). ^{13}C NMR

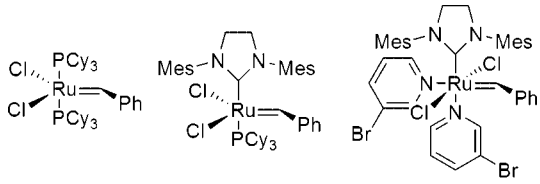

Figure 1. Grubbs' catalysts.

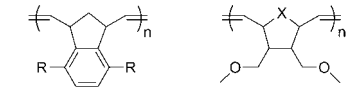

Figure 2. Structures of homopolymers.

Table 1. GPC Results of Homopolymerization

monomer	catalyst	time (h)	yield (%)	[M]/[Cat.]	M_n	PDI
4	**13**	24	25	180	12 700	1.10
6	**13**	24	80	345	67 800	1.18
9	**13**	2	90	200	53 400	1.04
9	**15**	1	98	375	60 100	1.11
12	**13**	6	70	245	33 400	1.18
12	**15**	2	97	180	38 100	1.05

(75 MHz, $CDCl_3$): 135.37, 72.97, 58.80, 49.18, 45.62, 41.50. HR-MS (ESI): calcd for $C_{11}H_{18}O_2$ $[M + Na]^+$, 205.120; found 205.120.

General Procedure for Homopolymerizations. In a nitrogen-filled drybox, a solution of the monomer (**4**, **5**, **6**, **9**, or **12**) in CH_2Cl_2 (0.1 g/mL concentration) was added in one portion to the vigorously stirred solution, including the desired amount of catalyst (**13**−**15**) in CH_2Cl_2. The reaction mixture was stirred at room temperature for various periods of time before quenching with ethyl vinyl ether. The reaction mixture was poured into methanol or hexane to precipitate the polymer, which was dried in vacuo.

Poly(4). The polymer was obtained as a white solid (25%) for 24 h reaction using catalyst **13**. ^{1}H NMR (500 MHz, CD_2Cl_2): δ 7.16, 6.90 (br, 8H), 4.94 (br, 2H), 4.45, 3.97 (br, 2H), 2.40, 1.55 (br, 2H). ^{13}C NMR (125 MHz, CD_2Cl_2): 142.54, 131.79, 129.48, 128.50, 127.71, 126.56, 125.60, 46.97, 43.49.

Poly(6). The polymer was obtained as a white solid (80%) for 24 h reaction using catalyst **13**. ^{1}H NMR (500 MHz, CD_2Cl_2): δ 7.44, 6.28 (br, 8H), 5.29 (br, 2H), 4.58, 3.94 (br, 2H), 2.57, 1.62 (br, 2H). ^{13}C NMR (125 MHz, CD_2Cl_2): 152.90, 142.62, 142.12, 133.45, 127.30, 125.34, 112.09, 109.11, 47.41, 43.20.

Poly(9). The clear tacky polymer was obtained (90%) for 2 h reaction using catalyst **13**. ^{1}H NMR (500 MHz, $CDCl_3$): δ 5.72, 5.55 (br, m, 2H), 4.53, 4.22 (br, m, 2H), 3.48 (br, m, 4H), 3.33 (s, 6H), 2.26 (br, 2H). ^{13}C NMR (125 MHz, CD_2Cl_2): 133.78, 82.17, 77.43, 77.09, 71.23, 70.98, 70.63, 70.41, 59.12, 48.38, 47.95, 47.60, 47.29. The yield was 98% for 1 h reaction using catalyst **15**.

Poly(12). The polymer was obtained as a white solid (70%) for 6 h reaction using catalyst **13**. ^{1}H NMR (500 MHz, $CDCl_3$): δ 5.38 (br, 2H), 3.38 (br, t, 4H), 3.29 (s, 6H), 3.00, 2.69 (br, m, 2H), 2.31 (br, 2H), 1.93, 1.38 (br, m, 2H). ^{13}C NMR (125 MHz, $CDCl_3$): 131.96, 71.57, 71.35, 71.22, 58.73, 45.82, 44.19, 40.76, 39.60, 38.90. The yield was 97% for 2 h reaction using catalyst **15**.

General Procedure for Block Copolymerizations. In a nitrogen-filled drybox, a solution of the first monomer **9** or **12** in CH_2Cl_2 (0.1 g/mL concentration) was added in one portion to the vigorously stirred solution including desired amount of catalyst (**13** or **15**) in CH_2Cl_2. The reaction mixture was stirred at room temperature for 2 h (6 h for monomer **12** when catalyst **13** was used) before adding second monomer solution of **4**, **5**, or **6** in CH_2Cl_2 (0.1 g/mL concentration). A small sample was taken just before the second monomer solution addition for GPC analysis. The copolymerization was allowed to stir another 22 h and quenched by addition of a drop of ethyl vinyl ether. The reaction mixture was poured into methanol or hexane to precipitate the copolymer, which was dried in vacuo. The polymerization yields varied from 65% to 96%. All protons and carbons of each block in copolymers corresponded to those of the appropriate homopolymers in ^{1}H NMR and ^{13}C NMR spectra.

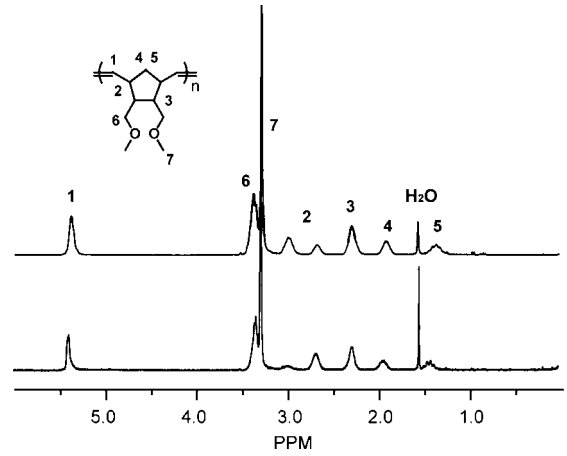

Figure 3. ^{1}H NMR spectra in $CDCl_3$ of poly(**12**) polymerized with **15** (top) and **13** (bottom).

General Procedure for Hydrogenation of Polymers. In a typical experiment, a polymer (50 mg) was dissolved in CH_2Cl_2 (1 mL), and then ethanol (10 mL), $CuSO_4$ (0.02 g, 0.08 mmol), and hydrazine (0.1 mL, 3.2 mmol) were added to the reaction flask. Air was slowly bubbled through overnight at room temperature and then filtered. After ethanol was removed, the mixture was extracted with CH_2Cl_2, and the organic portions were combined, washed with brine, and dried over magnesium sulfate. Evaporation of the solvent under reduced pressure afforded a tacky polymer. A literature procedure using tosyl hydrazide[22] was also used for hydrogenation of polymers. Since the aliphatic protons of both blocks of the copolymers had overlapping chemical shifts, it was difficult to isolate and assign the peaks.

Hydrogenated Poly(4). ^{1}H NMR (500 MHz, $CDCl_3$): δ 7.24, 6.99 (br, 8H), 3.36 (br, 2H), 1.81 (br, 1H), 1.44 (br, 3H), 1.00 (br, 2H). ^{13}C NMR (125 MHz, CD_2Cl_2): 146.19, 142.84, 131.00, 129.92, 127.50, 125.56, 125.36, 44.44, 42.47, 35.64, 33.84.

Hydrogenated Poly(6). ^{1}H NMR (500 MHz, $CDCl_3$): δ 7.34, 6.35 (br, 8H), 3.39 (br, 2H), 2.14, 1.58 (br, 6H). ^{13}C NMR (125 MHz, CD_2Cl_2): 153.56, 144.50, 141.90, 126.31, 125.30, 111.73, 107.55, 44.54, 42.65, 36.14, 33.48.

Hydrogenated Poly(9). ^{1}H NMR (300 MHz, $CDCl_3$): δ 3.70 (br, m, 2H), 3.43 (br, m, 4H), 3.32 (br, s, 6H), 2.16 (br, 2H), 1.60 (br, 4H). ^{13}C NMR (125 MHz, $CDCl_3$): 81.10, 80.98, 80.81, 71.47, 58.95, 46.44, 45.99, 32.00.

Hydrogenated Poly(12). ^{1}H NMR (300 MHz, $CDCl_3$): δ 3.36 (br, m, 4H), 3.31 (br, s, 6H), 2.23 (br, m, 2H), 2.03 (br, m, 1H), 1.90 (br, 2H) 1.48 (br, m, 2H), 1.06 (br, 1H), 0.93 (br, m, 2H). ^{13}C NMR (125 MHz, $CDCl_3$): 71.36, 58.83, 44.60, 40.96, 38.61, 30.49.

Results and Discussion

Monomer Synthesis. A series of norbornene derivatives having thiophene (**4**), bithiophene (**5**), and furan (**6**) moieties were synthesized as monomers for electroactive block copolymers (Scheme 2). A Diels−Alder reaction between 1,3-cyclopentadiene and 1,4-benzoquinone afforded the compound **1**. Without purification, **1** was tautomerized to diol **2**, which was subsequently converted into **3** using perfluoro-1-butanesulfonyl floride.[13] Compounds **4**, **5**, and **6** were obtained from Stille coupling reaction between aryl dinonaflate **3** and suitably stannylated heterocyclic precursors.

We followed the literature syntheses of monomers **9**[12] and **12**[14] as described in Scheme 3. Diels−Alder reactions of furan

Scheme 4

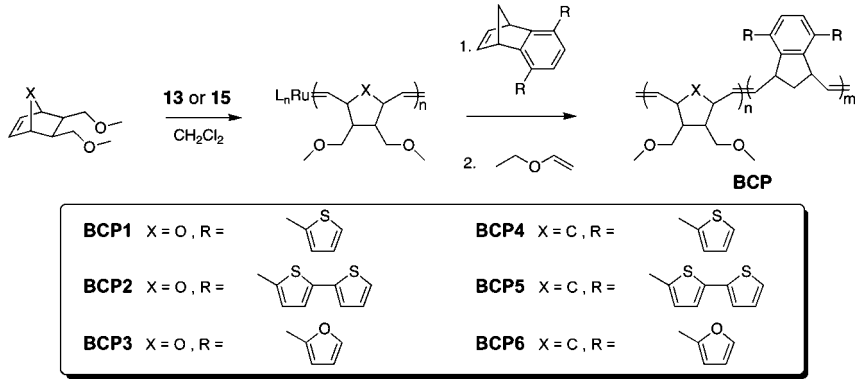

Table 2. GPC Results of Block Copolymerizations

polymer	M_1	M_2	catalyst	$[M_1]/[M_2]/[Cat.]$	M_n	PDI	*n/m*
BCP1	**9**	**4**	**13**	210/50/1	58 600	1.02	290/15
BCP2	**9**	**5**	**13**	220/20/1	53 700	1.03	270/10
BCP3	**9**	**6**	**13**	220/110/1	69 200	1.10	300/50
BCP4	**12**	**4**	**13**	220/60/1	59 300	1.05	270/35
BCP5	**12**	**5**	**15**	210/10/1	47 800	1.06	240/10
BCP6	**12**	**6**	**15**	190/50/1	53 800	1.08	240/35

Table 3. T_gs of Block Copolymers

polymer	T_g (°C) before hydrogenation	T_g (°C) after hydrogenation
BCP1	26.5	5.4
BCP2	22.2	2.3
BCP3	21.3	4.8
BCP4	50.2	42.2
BCP5	66.4	44.6
BCP6	64.2	42.1

or 1,3-cyclopentadiene and maleic anhydride afforded **7** (exo major) or **10** (endo major), respectively. These adducts were reduced with lithium aluminum hydride to afford diol **8** and **11**. A double Williamson ether synthesis in the presence of excess sodium hydride followed by treatment with methyl iodide resulted in the diether monomers **9** and **12** as viscous oils after vacuum distillation.

Homopolymerizations. Homopolymers of each monomer were synthesized to examine reactivity with ROMP catalysts before the synthesis of block copolymers. Homopolymerization reactions of monomers (**4**, **5**, **6**, **9**, and **12**) with Grubbs' catalysts, **13**, **14**, and **15** (Figure 1) were examined in CH_2Cl_2 at room temperature, and the polymers poly(**4**), poly(**5**), poly(**6**), poly(**9**), and poly(**12**) (Figure 2) were isolated by precipitation

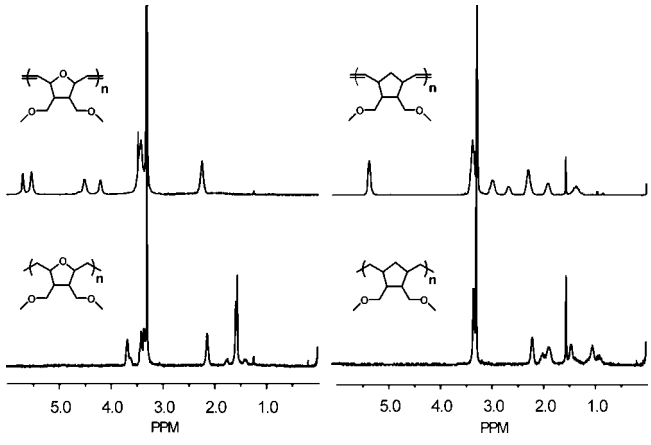

Figure 4. ^{1}H NMR spectra in $CDCl_3$ of poly(**9**) (top left), hydrogenated poly(**9**) (bottom left), poly(**12**) (top right), and hydrogenated poly(**12**) (bottom right).

Scheme 5

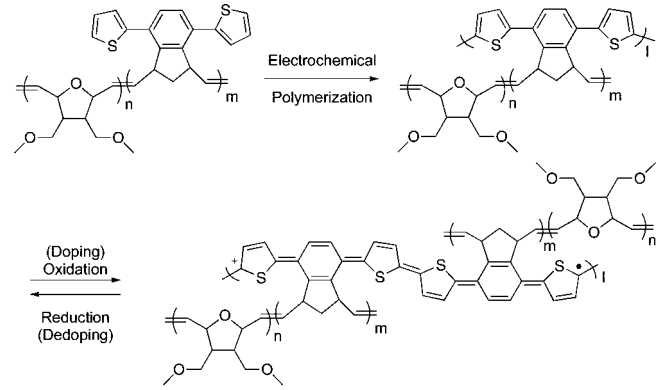

into methanol or hexane. We found that catalyst **13** polymerized *exo*-7-oxanorbornene derivative **9** quantitatively within 1 h, but **13** polymerized *endo*-norbornene derivative **12** more slowly (70% yield for a 6 h reaction). Previous studies have shown that *exo* isomers react faster than the corresponding *endo* isomers for the ROMP of norbornene derivatives due to steric interactions between the polymer chains and the approaching monomer.[15] We also found that monomers having sulfur (**4** and **5**) were slow to polymerize and could not be driven to completion with **13** possibly because the catalyst was deactivated by coordination to the sulfur center.[16] In the case of **5**, only oligomers (M_n = 2100, PDI = 1.07) were obtained, apparently due to its poor solubility and sluggish polymerization. It is known that catalyst **14** displays higher activity than catalyst **13** toward olefinic substrates[17] and is tolerant of the substrates containing sulfur atoms.[16] Consistent behavior was observed with our monomers, and higher molecular weight polymers (an insoluble polymer for monomer **5**) with broader PDIs were obtained using **14**. Grubbs has reported a next generation catalyst **15** which has superior initiation properties over **14** for the metathesis of simple olefins and is easily synthesized in one step from **14**.[18] We also polymerized all monomers with this catalyst. The monomers having heterocyclic ring (**4**, **5**, and **6**) precipitated during polymerization, while poly(**9**) and poly(**12**) were synthesized in a controlled polymerization with living characteristics within 1 h by **15**. Table 1 summarizes the GPC results of the homopolymerizations.

Poly(**12**) polymerized with different catalysts had different configurations of double bonds (Figure 3). Consistent with the ^{1}H NMR spectral data previously reported,[19] a 75:25 ratio of trans to cis olefins was revealed by integration of the signals for H(2) for the poly(**12**) polymerized from **13** (Figure 3, bottom). However, a 33:67 ratio of trans to cis olefins was observed for poly(**12**) polymerized from **15** (Figure 3, top). The stereochemistry of poly(**9**) was insensitive to the catalyst used and the ratio was approximately a 50:50 ratio of trans to cis olefins.

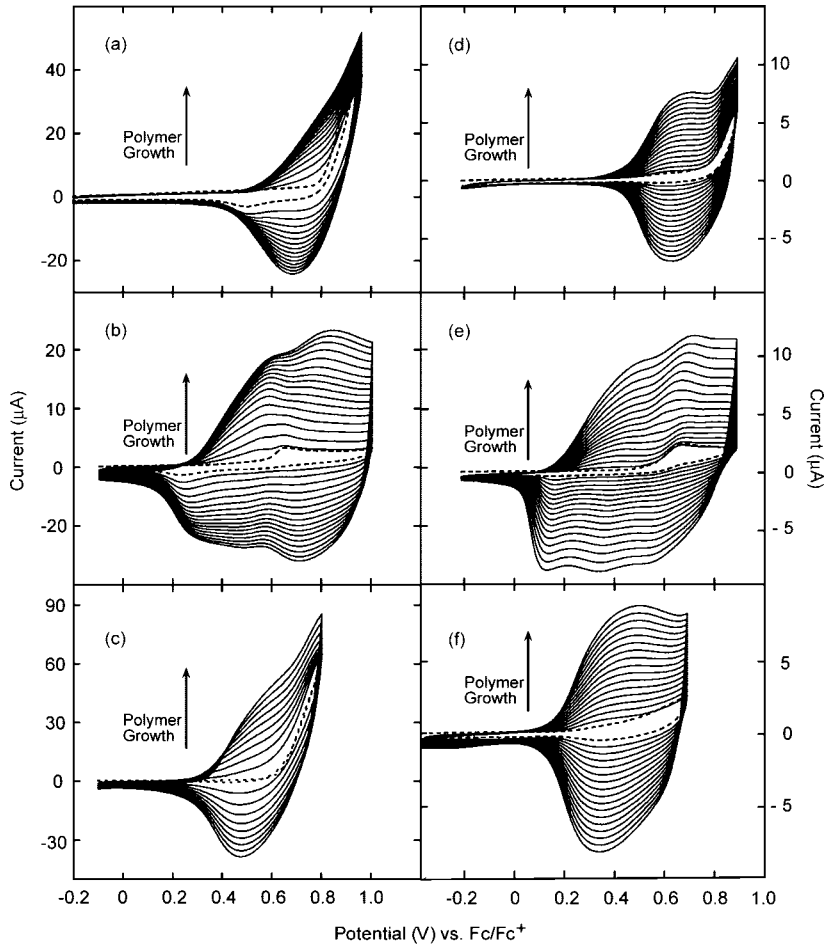

Figure 5. Electropolymerizations of monomers **4** (a), **5** (b), and **6** (c) and block copolymers **BCP1** (d), **BCP2** (e), and **BCP3** (f) on Pt button electrodes in CH_3CN (for monomers **4**−**6**) or CH_2Cl_2 (for polymers **BCP1**−**BCP3**) solutions containing 0.1 M $TBAPF_6$. Dotted lines represent the first scans, and all CVs were obtained at scan rate of 100 mV/s.

Block Copolymerizations. Based on the homopolymerization of monomers, the synthesis of block copolymers was accomplished by adding monomers **4**−**6** to the growing polymer chain of poly(**9**) that was initiated by catalyst **13** (Scheme 4). Catalyst **13** afforded soluble copolymers with narrow PDIs. In the case of polymerization of **9**, the polymerization was allowed to proceed for 2 h at room temperature, and then solutions of **4**, **5**, or **6** were added. A small amount of sample was taken from the initial polymerization just before the second monomer addition for GPC analysis. After stirring for another 22 h, the reaction mixture was quenched with ethyl vinyl ether and precipitated into hexanes to afford copolymers as pale yellow (**BCP1**), yellow (**BCP2**), or white (**BCP3**) solids.

The synthesis of block copolymers based on **12** and **4**−**6** were also performed in the same manner. Catalyst **15** was used for the synthesis of these block copolymers because **13** was ineffective for the polymerization of **12**. However, **BCP4** synthesized by **15** displayed apparent high molecular weights with low solubility. Therefore, we used **13** to synthesis soluble forms of **BCP4**.

Table 2 summarizes the GPC results of the block copolymers. The relative ratios of each copolymer were determined by GPC or ^{1}H NMR spectroscopy. As the ratio of monomer **9** or **12** increased, the copolymer became qualitatively more elastic. The elastomeric properties of poly(**9**) and poly(**12**) provides for qualitatively improved mechanical properties and reduced brittleness. Although the polymerization of the second block was not completely living, the PDIs of the resulting polymers were narrow.

Hydrogenation of Polymers. The as-synthesized block copolymers are not indefinitely stable in air. The polymers when stored under ambient became insoluble for weeks while the polymers stored under N_2 were still soluble. It is likely that the unsaturated C═C double bonds and tertiary C−H bonds, which are both allylic and benzylic, are responsible for the oxidation and degradation of polymers.[20] **BCP1**−**BCP3** that have tetrahydrofuran groups are also prone to oxidation due to additional activation of tertiary allylic C−H bonds by the oxygen. The double bonds could be also affected when the polymers are chemically or electrochemically oxidized. We therefore decided to remove the double bonds by hydrogenation to solve these problems. Hydrogenation of the polymer backbone was carried out using hydrazine and copper sulfate in the mixture of ethyl alcohol and CH_2Cl_2 with slow bubbling of air through the mixture.[21] Refluxing in xylenes with tosyl hydrazide[22] was also an effective hydrogenation method for our block copolymers and gave similar results. The olefin protons completely disappeared after hydrogenation when analyzed by ^{1}H NMR spectroscopy (Figure 4).

The hydrogenated polymers displayed higher molecular weights and broader PDIs. Hydrogenation was also found to lower the T_g's of polymers due to increased freedom of rotation in the backbone (Table 3). **BCP4** experiences about 15 deg decrease in T_g as compared with **BCP5** and **BCP6**. As mentioned before, poly(**12**) in **BCP4** had different stereochemical composition since it was polymerized with **13**. T_g of **BCP4** polymerized with **15** was 73.6 °C. We should mention that observed T_gs are mainly for the first blocks (poly(**9**) or poly(**12**))

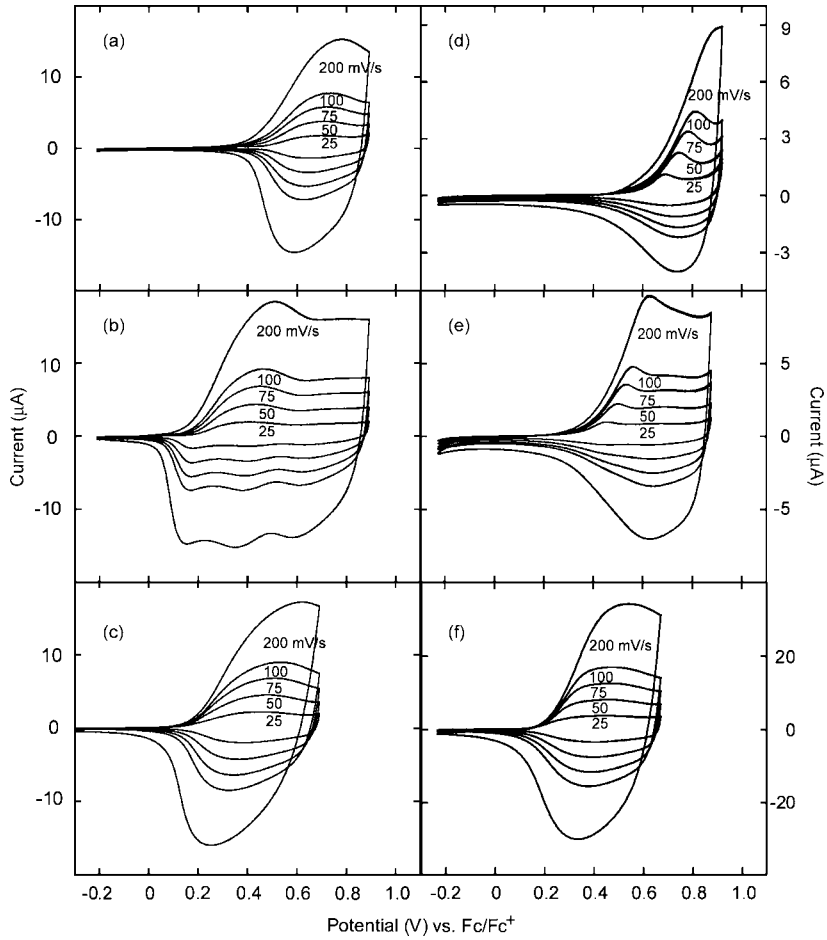

Figure 6. CVs of block copolymers (**BCP1** (a), **BCP2** (b), and **BCP3** (c)) and hydrogenated block copolymers (**BCP1** (d), **BCP2** (e), and **BCP3** (f)) on Pt button electrodes in 0.1 M $TBAPF_6$ of CH_2Cl_2 solution. Polymer film CVs were obtained at 25−200 mV/s.

of block copolymers. Homopolymers, poly(**4**) and poly(**6**), have T_gs of 250.0 and 245.0 °C, respectively. However, we could not observe other T_gs for the block copolymers even when heated to 350 °C.

Electrochemistry. All electropolymerizations to create interpenetrating polymer networks were performed by electrodeposition of compounds on Pt button electrodes under swept potential conditions (Scheme 5). In the first step of electropolymerization, neutral monomers are oxidized to radical cations at the electrode. Then the monomers dimerize (mainly at the α-position) and protons are eliminated, forming a neutral species. Since the dimer with its greater conjugation is more easily oxidized than the monomer, it is immediately reoxidized to the cation, which can further couple with other cations to extend the chain. The process of oxidative coupling and proton elimination continues until insoluble oligomers form and are deposited on the electrode surface.

First, electropolymerizations of three electroactive monomers (**4**−**6**) were performed in CH_3CN solutions containing ca. 5 mM of each monomer and 0.1 M of $TBAPF_6$ as an electrolyte. Figures 5a−c depict the anodic polymerization of monomers **4**−**6**. The irreversible oxidative peaks in the first scans (dotted lines in Figure 5) are attributed to the oxidation of heterocyclic units. The anodic peaks corresponding to the oxidation of the conducting polymers typically appeared after the second cycle. The increase in current after each potential scan indicates polymer film growth on the working electrode. The monomer possessing a bithiophene moiety, **5**, oxidized at the lowest potential (0.60 V) and the oxidation onset value for the monomer having thiophene, **4**, was higher than that of the monomer having furan, **6** (0.80 and 0.62 V, respectively). This is likely due to the larger size of sulfur compared to oxygen, resulting in greater steric interactions and a nonplanar conformation for the phenyl−thienyl linkeges.[23]

Electropolymerizations of homopolymers (poly(**4**)−poly(**6**)) and block copolymers (**BCP1**−**BCP6**) were also carried out. Because of solubility problems, electropolymerization of polymers were performed in CH_2Cl_2 solutions containing ca. 4 μM of electroactive unit (2−3 mg/mL of each polymer) and 0.1 M of $TBAPF_6$ as an electrolyte. CVs for homopolymers' electropolymerization showed similar peaks to those observed for block copolymers. The oxidation potentials obtained for the block copolymers are nominally different from those obtained for the monomers in part because of a difference in the solvent used for both experiments (Figure 5). Specifically, the half-wave potential for Fc/Fc^+ in CH_2Cl_2 is ca. 0.15 V higher than that in CH_3CN; the potential values obtained in CH_3CN are higher than those obtained in CH_2Cl_2 when Fc/Fc^+ is used as the internal reference.

Both interchain and intrachain cross-linking are likely in the precursor polymers, even though we cannot quantitatively determine the extent of each. The peak current increases indicate a constant growth of the polymer films with repeated scans and demonstrate that these copolymers have sufficient conductivities to serve as a working electrode even though the conducting blocks are much shorter than nonconducting blocks. If the polymer was insulating or polymerization only proceeded at the electrode surface, there would be a decrease in the rate of film growth.[3] However, attempts to obtain in situ conductivities were

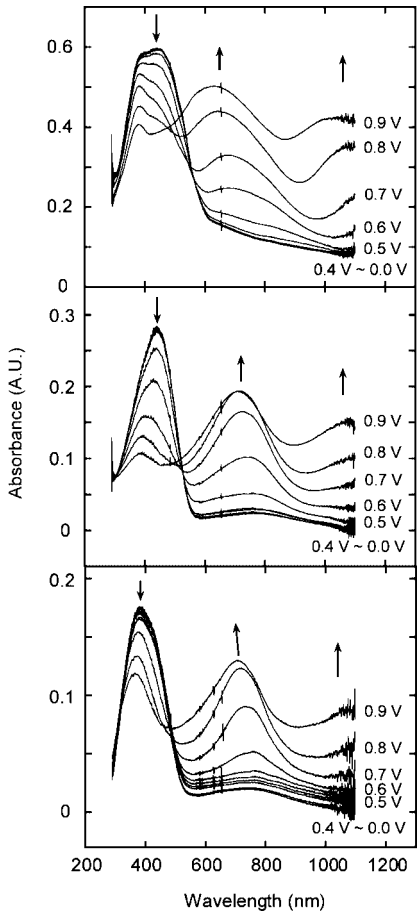

Figure 7. UV−vis absorption spectra of **5** (top), **BCP2** (middle), and hydrogenated **BCP5** (bottom) on ITO-coated glass electrodes in CH_2Cl_2 solution containing 0.1 M $TBAPF_6$ between 0.0 and 0.9 V (vs Ag/Ag^+).

unsuccessful due to poor adhesion of polymer films on interdigitated microelectrodes.

After electropolymerization, the electrode coated with a polymer was washed with CH_2Cl_2 and placed into a polymer-free solution of 0.1 M $TBAPF_6$ in order to examine the electrochemical processes of the electrodeposited polymer. Figure 6 compares the CVs of the block copolymers and their hydrogenated polymers of **BCP1**−**BCP3**. The linear increase of the peak current with respect to the scan rate establishes that the observed redox processes arise from surface-deposited materials. The CVs for the electropolymerized films, especially **BCP2**, exhibit reversible redox waves over a broad range of potentials, findings consistent with the highly delocalized nature of π-extended systems. Glenis et al. reported that with the electrolyte PF_6^- polyfuran could not be electropolymerized because of strong association of this dopant with the oxidized polymer, which results in irreversible chemical reactions.[24] However, monomer **6** and polymers (**BCP3** and **BCP6**) which have a furan moiety were found to electropolymerize in the presence of $TBAPF_6$, and the CVs of the resulting electrodeposited polymer films displayed stable electroactivities.

We had expected that hydrogenation of double bonds in the polymer backbone would not alter the electrochemical properties of original polymers since electroactive moieties were not affected by hydrogenation. Hydrogenated block copolymers retained the stable electroactivity; however, they display slightly higher oxidation onset values and narrower peak widths compared with their original polymers (Figures 6d−f). The CV of hydrogenated **BCP1** changed the most since it had the highest oxidation potential which may produce trapped sites inaccessible to counterion transport.[23] The general effects of hydrogenation on the electrochemical behavior are likely the result of (a) an increase in the nonpolar nature of the materials, which does not favor a highly charged doped state, and (b) increased steric bulk in the polymer backbone, which may limit the ability of oxidized pendant thienyl and furyl groups to couple.

BCP4−**BCP6**, which were polymerized using **15**, displayed poorer electrochemical characteristics (see Supporting Information). Most noteworthy is **BCP4** synthesized using **15**, which did not show any electroactivity, possibly because of decreased counterion mobility in the higher molecular weight and potentially cross-linked structure. **BCP4** polymerized using **13** exhibits similar electrochemistry to hydrogenated **BCP1**. On the hand, hydrogenated **BCP5** and **BCP6** showed similar CVs to hydrogenated **BCP2** and **BCP3**, respectively.

Spectroelectrochemistry. Reversible, uniform color changes were observed during redox cycles of the conducting polymer films. Figure 7 shows representative in situ measurements of the UV−vis absorption of electropolymerized polymers having bithiophene moieties deposited onto ITO-coated glass electrodes. Each of the polymers in the series exhibits similar behavior. At first, there is no long wavelength absorbances in the spectrum with absorption onset at 620 nm (2.0 eV) for **5** and 550 nm (2.3 eV) for block copolymers **BCP2** and hydrogenated **BCP5**. The onset of the optical absorptions corresponds to π to π^* transitions that give the approximate band gaps of the conducting polymers. The applied potential was increased 0.1 V intervals, and a spectrum was recorded at each potential up to 0.9 V (vs Ag/Ag^+). New, lower energy absorbance peaks become apparent with applied potential above 0.5 V (vs Ag/Ag^+). The absorbance for the π to π^* transitions, with maximum around 400 nm, continues to decrease while the absorbances at lower energies continue to increase upon further oxidation. A peak at near 1100 nm is commonly attributed to a transition from the valence band to intermediate bipolaron states for intrinsically conducting polymers. As expected, hydrogenation did not affect the electronic band structures. On the basis of these results and the electrochemical behavior, it is clear that oxidation of the block copolymer produces a network of conducting polymer chains.

Conclusions

We have utilized ROMP to synthesize novel precursor block copolymers having heterocyclic moieties to form conducting polymers. These block copolymers, which have electroactive blocks, showed stable electroactivity after subsequent electropolymerization. Hydrogenation of polymer backbones increased the polymers' stability without dramatically reducing electrochemical properties. These types of materials can be used to prepare nanostructures and may further applied in the formation of actuators and electrochromic devices.

Acknowledgment. This research was supported by the U.S. Army through the Institute for Soldier Nanotechnologies under Contract W911NF-07-D-004 with the U.S. Army Research Office.

Supporting Information Available: CVs of monomers (**4**, **5**, and **6**), homopolymers (**poly(4)**, **poly(5)**, and **poly(6)**), and block copolymers (**BCP4**, **BCP5**, and **BCP6**, their hydrogenated polymers) and the molecular weight of first blocks of block copolymers. This material is available free of charge via the Internet at http://pubs.acs.org.

References and Notes

(1) (a) *Handbook of Conducting Polymers*, 2nd ed.; Skotheim, T. A., Elsenbaumer, R. L., Reynolds, J. R., Eds.; Marcel Dekker: New York, 1998. (b) *Handbook of Organic Conductive Molecules and Polymers*; Nalwa, H. S., Ed.; Wiley: New York, 1997; Vols. *1*− *4*.

(2) (a) Roncali, J. *Chem. Rev.* **1997**, *97*, 173–205. (b) Kraft, A.; Grimsdale, A. C.; Holmes, A. B. *Angew. Chem., Int. Ed.* **1998**, *37*, 402–428. (c) *Handbook of Oligo- and Polythiophenes*; Fichou, D., Ed.; Wiley-VCH: New York, 1999. (d) Roncali, J. *J. Mater. Chem.* **1999**, *9*, 1875–1893. (e) Kanazawa, K. K.; Diaz, A. F.; Geiss, R. H.; Gill, W. D.; Kwark, J. F.; Logan, A.; Rabolt, J. F.; Street, G. B. *J. Chem. Soc., Chem. Commun.* **1979**, 854–855.
(3) (a) Jang, S.; Sotzing, G. A. *Macromolecules* **2002**, *35*, 7293–7300. (b) Jang, S.; Sotzing, G. A.; Marquez, M. *Macromolecules* **2004**, *37*, 4351–4359.
(4) Xia, C.; Fan, X.; Park, M.; Advincula, R. C. *Langmuir* **2001**, *17*, 7893–7898.
(5) Xia, C.; Advincula, R. C. *Chem. Mater.* **2001**, *13*, 1682–1691.
(6) Watson, K. J.; Wolfe, P. S.; Nguyen, S. T.; Zhu, J.; Mirkin, C. A. *Macromolecules* **2000**, *33*, 4628–4633.
(7) Jang, S.; Marquez, M.; Sotzing, G. A. *J. Am. Chem. Soc.* **2004**, *126*, 9476–9477.
(8) Förster, S.; Plantenberg, T. *Angew. Chem., Int. Ed.* **2002**, *41*, 688–714.
(9) Albagli, D.; Bazan, G.; Wrighton, M. S.; Schrock, R. R. *J. Am. Chem. Soc.* **1992**, *114*, 4150–4158.
(10) Gilliom, L.; Grubbs, R. H. *J. Am. Chem. Soc.* **1986**, *108*, 733–742.
(11) Zhu, S. S.; Swager, T. M. *J. Am. Chem. Soc.* **1997**, *119*, 12568–12577.
(12) Manka, J. T.; Douglass, A. G.; Kaszynski, P.; Friedli, A. C. *J. Org. Chem.* **2000**, *65*, 5202–5206.
(13) Stang, P. J.; Hanack, L.; Subramanian, R. *Synthesis* **1982**, 85–126.
(14) Lynn, D. M.; Kanaoka, S.; Grubbs, R. H. *J. Am. Chem. Soc.* **1996**, *118*784–790.
(15) (a) Rule, J. D.; Moore, J. S. *Macromolecules* **2002**, *35*, 7578–7882. (b) Pollino, J. M.; Stubbs, L. P.; Weck, M. *Macromolecules* **2003**, *36*, 2230–2234.
(16) (a) Carlisle, J.; Fox, D. J.; Warren, S. *Chem. Commun.* **2003**, 2696–2697. (b) Spagnol, G.; Heck, M.; Nolan, S. P.; Mioskowski, C. *Org. Lett.* **2002**, *4*, 1767–1770.
(17) Sanford, M. S.; Love, J. A.; Grubbs, R. H. *J. Am. Chem. Soc.* **2001**, *123*, 6543–6554.
(18) Love, J. A.; Morgan, J. P.; Trnka, T. M.; Grubbs, R. H. *Angew. Chem., Int. Ed.* **2002**, *41*, 4035–4037.
(19) (a) Nomura, K.; Sagara, A.; Imanishi, Y. *Macromolecules* **2002**, *35*, 1583–1590. (b) Gilliom, L. R.; Grubbs, R. H. *J. Am. Chem. Soc.* **1986**, *108*, 733–742.
(20) Delaude, L.; Demonceau, A.; Noels, A. F. *Macromolecules* **1999**, *32*, 2091–2103.
(21) Brown, H. C.; Bakshi, R. K.; Singaram, B. *J. Am. Chem. Soc.* **1988**, *110*, 1529–1534.
(22) Scherman, O. A.; Kim, H. M.; Grubbs, R. H. *Macromolecules* **2002**, *35*, 5366–5371.
(23) Child, A. D.; Sankaran, B.; Larmat, F.; Reynolds, J. R. *Macromolecules* **1995**, *28*, 6571–6578.
(24) Glenis, S.; Benz, M.; LeGoff, E.; Schindler, J. L.; Kannewurf, R.; Kanatzidis, M. G. *J. Am. Chem. Soc.* **1993**, *115*, 12519–12525.

MA8006416